Charred forests increase snowmelt: Effects of burned woody debris and incoming solar radiation on snow ablation

Kelly E. Gleason,[1] Anne W. Nolin,[1] and Travis R. Roth[1]

Received 12 June 2013; revised 19 August 2013; accepted 20 August 2013; published 10 September 2013.

[1] We document effects of postfire forest conditions on snow accumulation, albedo, and ablation in the Oregon Cascades. We measured snow water equivalent, solar radiation, snow albedo, and snowpack surface debris at a pair of burned and unburned forest plots. Snow accumulation was greater in the burned forest; however, the snowpack disappeared 23 days earlier and had twice the ablation rate than in the unburned forest. Snow albedo was 40% lower in the burned forest during ablation, while approximately 60% more solar radiation reached the snow surface, driving a 200% increase in net shortwave radiation. Significant amounts of pyrogenic carbon particles and larger burned woody debris shed from standing charred trees accumulated on the snowpack and darkened its surface. Spatial analysis showed that across the Western U.S., 80% of all forest fires occurred in the seasonal snow zone, and were 4.4 times larger than fires outside the seasonal snow zone. **Citation:** Gleason, K. E., A. W. Nolin, and T. R. Roth (2013), Charred forests increase snowmelt: Effects of burned woody debris and incoming solar radiation on snow ablation, *Geophys. Res. Lett.*, *40*, 4654–4661, doi:10.1002/grl.50896.

1. Introduction

[2] In the montane western United States, most annual precipitation falls as snow [*Serreze et al*., 1999], yet rising temperatures have reduced snowpacks [*Abatzoglou*, 2011; *Brown and Mote*, 2009; *Knowles et al*., 2006; *Mote et al*., 2005; *Pederson et al*., 2013]. Key consequences of this have been increases in wildfire frequency, size, intensity, and duration across the western U.S. [*Westerling et al*., 2006]. Total burned area in the western U.S. is anticipated to increase [*Littell et al*., 2009; *Moritz et al*., 2012; *Westerling et al*., 2011] as a result of climate change and fire suppression [*Marlon et al*., 2012].

[3] Forest fire affects patterns of snow accumulation and ablation by reducing canopy interception, increasing light transmission, and modifying the surface energy balance [*Burles and Boon*, 2011; *Harpold et al*., 2013; *Winkler*, 2011]. Previous work showed that snow ablation rates are accelerated as much as 57% and snow disappeared 4–15 days earlier in a burned forest [*Burles and Boon*, 2011; *Skidmore et al*., 1994; *Winkler*, 2011], but these studies omitted measurements of burned debris and its effect on snow spectral albedo. The objective of this paper is to demonstrate how charred forests decrease snow albedo through debris deposition, and how when combined with increased solar radiation, this leads to earlier snow disappearance.

[4] Because snow is highly reflective in the visible wavelengths (400–700 nm), even a small decrease in visible albedo will dramatically increase net shortwave radiation [*Dozier et al*., 2009]. Previous work has shown that light absorbing impurities in snow, such as dust and soot, can lead to substantial radiative heating and faster snow melt rates [*Flanner et al*., 2009; *Painter et al*., 2012; *Painter et al*., 2007; *Skiles et al*., 2012]. Compared with mineral dust, carbon soot is an order of magnitude more effective at absorbing solar energy in the visible wavelengths [*Warren and Wiscombe*, 1980]. Although far more coarse than dust and soot, debris from the forest canopy accumulates on the snowpack and reduces albedo [*Hardy et al*., 2000; *Melloh et al*., 2001]. For decades after a fire, burned woody debris (BWD) including pyrogenic carbon [*Preston and Schmidt*, 2006], charcoal, charred woody detritus, and partially charred needles, cones, and bark are shed from standing burned trees onto the snowpack [*Dunn and Bailey*, 2012]. While it is visibly apparent that BWD darkens the snow surface (Figure 1), the effects on snow spectral albedo and snowpack ablation have not been quantified. This investigation provides the first measurements of snow spectral albedo and snow surface BWD in a burned forest, and provides evidence for the impacts of wildfire on snow accumulation and ablation.

2. Site Description

[5] The study area is located in the Oregon High Cascades at an elevation of 1750 m, in the headwaters of the McKenzie River Basin, a major tributary to the Willamette River. This area receives approximately 3000 mm of precipitation a year, most of which falls as snow from November to April [*Taylor and Hannan*, 1999]. In late summer 2011, the Shadow Lake Fire burned 42 km^2 of High Cascades mixed conifer forest [*Franklin and Dyrness*, 1973] in the Willamette and Deschutes National Forests (Figure 2). About 50% of the area burned with moderate-to-high burn severity, with near total loss of forest canopy (Figure 3). This location serves as an ideal field laboratory for our paired study of snowpack dynamics and snow albedo in a severely burned forest (BF) plot and in an adjacent, unburned forest (UF) plot.

3. Research Methods

3.1. Measuring Postfire Snow Spectral Albedo and Net Radiation

[6] Snow spectral albedo was measured every 20 m along a 200 m transect in the burned and unburned study sites using an Analytical Spectral Devices Full-Range Portable Field

[1]College of Earth, Ocean, and Atmospheric Sciences, Oregon State University, Corvallis, Oregon, USA.

Corresponding author: K. E. Gleason, College of Earth, Ocean, and Atmospheric Sciences, Oregon State University, 104 Wilkinson Hall, Corvallis, OR 97331, USA. (gleasoke@science.oregonstate.edu)

0094-8276/13/10.1002/grl.50896

Figure 1. Burned woody debris (BWD)—pyrogenic carbon, charred woody detritis, burned branches, cones, and bark—accumulated on the snowpack surface.

Spectrometer™ (ASD-FR) equipped with a cosine receptor, mounted on a 110-cm long horizontally leveled rod. The ASD-FR has a spectral resolution of 10 nm over a spectral range of 350-2500 nm. Measurements were made on 25 March 2013 (accumulation period) and 04 May 2012 and 01 May 2013 (ablation period). All spectral measurements were made within one hour of solar noon under clear sky conditions.

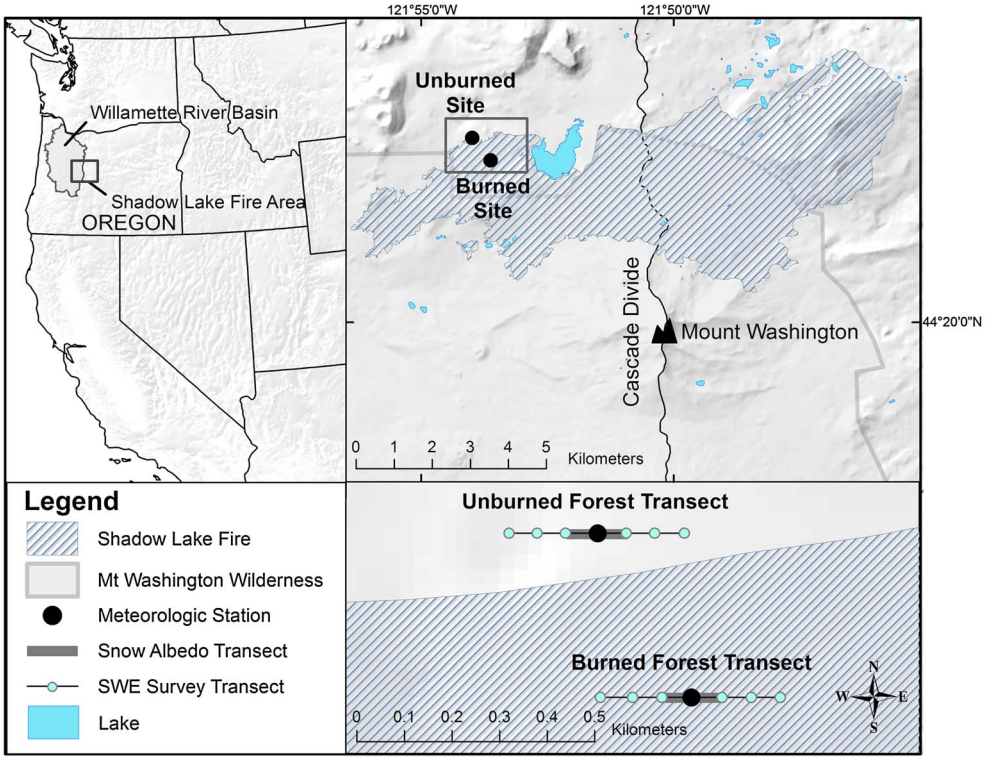

Figure 2. Burned and unburned forest sites are located in the Shadow Lake Fire area.

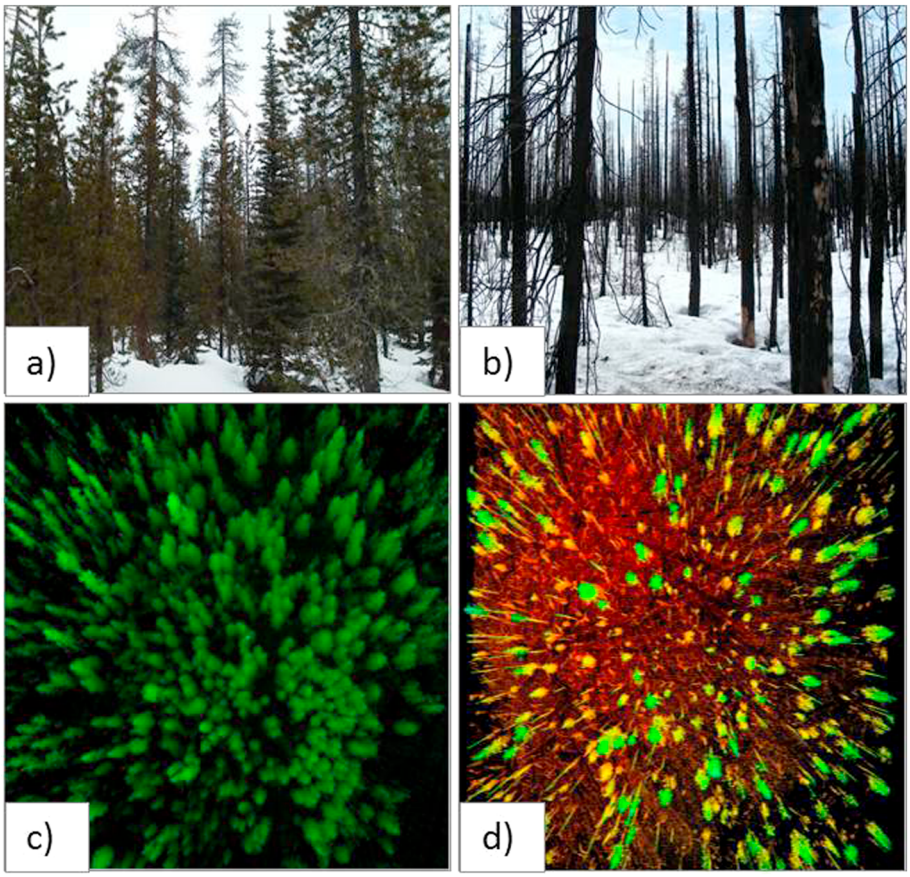

Figure 3. (a) Unburned and (b) burned forests, 4 May 2012; aerial representation of (c) unburned forest and (d) burned forest structure as determined by TLS surveys, colored by relative elevation (red = lowest elevation and green = highest elevation in scan area).

[7] Solar radiation was measured from upward- and downward-facing LI-COR™ 200 s pyranometers installed at 5 m above ground on a tower located at the transect center in each plot. The pyranometers have a spectral range of 400–1100 nm and a 180º field-of-view. Power supply issues at both sites restricted the coincident radiation data to two periods: 04–27 February (accumulation period) and 8 May–01 July (ablation period). Hourly mean incoming and outgoing solar radiation values were calculated using all snow-free data for solar elevation angle >30°. Hourly mean broadband snow albedo was calculated, when snow depth was greater than 30 cm, as the ratio of outgoing to incoming solar radiation.

[8] We quantified changes in net shortwave radiation using pyranometer-measured broadband albedo and ASD-FR-measured snow spectral albedo. For comparison with the pyranometer data, we convolved the ASD-FR measurements over the spectral range of the pyranometer.

3.2. Snow Debris Concentration and Spectral Reflectance Characterization

[9] At spectral albedo measurement locations, we collected a snow surface sample (0.5 m^2 area × 0.03 m depth) for subsequent filtration. Snow samples were melted in a 30°C oven and filtered using pre-weighed Whatman™ glass fiber filters (55 mm and 0.7 µm pore size) with vacuum filtration. Sampled filtrate and oven-dried debris were weighed to determine the mass of debris per unit mass of snow water equivalent. Filters were retained for measurement of spectral reflectance of the debris. Spectral reflectance factors of filtered debris samples were measured relative to a calibrated Spectralon® target using the ASD-FR equipped with an 8° foreoptic on 7 September 2012. Debris consisted of a thick (>5 mm) layer completely covering the filter.

3.3. Snow Surveys and Forest Structure Measurements

[10] We measured snow depth and snow water equivalent (SWE) along 0.5 km transects in both plots. Monthly measurements were made from December 2011 to April 2012, and biweekly measurements were made from 15 April 2012 until snow disappearance. Snow depth was measured every 10 m, and SWE was measured every 100 m. At each SWE measurement location, snow surface samples were collected for debris filtration as described above.

[11] Forest structure within each plot was characterized using a Riegl VZ400™ terrestrial laser scanner (TLS). TLS metrics including tree height, crown radius, forest density; and aerial visualizations were produced within a 250 m radius using Cyclone™ and ArcGIS™ (Figure 3). We also quantified canopy closure every 50 m along each transect using hemispherical digital photos (Nikon Coolpix 995 w/ leveled fish-eye lens) and Gap Light Analyzer 2.0 [*Frazer et al.*, 1999].

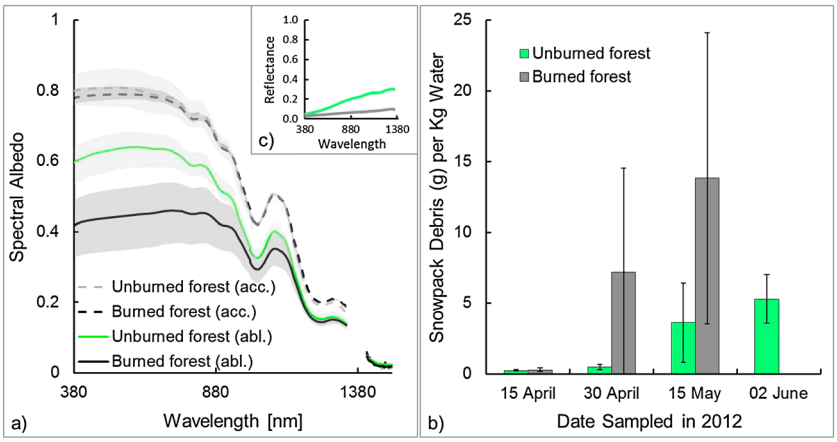

Figure 4. (a) Mean ASD-FR-measured snow spectral albedo during accumulation (acc. 25 March 2013) and ablation (abl. 4 May 2012), shaded grey areas indicate range of measurements. (b) Mean debris concentrations in ablation season snow samples; bars indicate one standard deviation. (c) Reflectance factors of debris filtered from ablation season snow samples.

3.4. Geospatial Analysis

[12] To provide a broader spatial context for our field study, we mapped coincident areas of wildfire, seasonal snow, and forest cover over the western U.S. using ArcGIS. We used data from the Moderate Resolution Imaging Spectroradiometer (MODIS) including MOD10A2 500 m 8 day maximum snow covered area product [*Hall et al*., 2006] and the MOD44B 250 m vegetation continuous fields (VCF) product [*DiMiceli et al*., 2011] for years 2000–2012. Based on *Robinson and Frei* [2000], we selected 15 January to represent the maximum winter snow cover extent for the western U.S., and for each year used the MOD10A2 image nearest that date. Snow cover frequency in each MODIS pixel was calculated as the ratio of the number of years when snow was observed relative to the number of years in the data record. The seasonal snow zone was defined by pixels with snow cover frequency of at least 25%. Forest cover pixels were identified using the MODIS VCF product that we aggregated to 500 m to match the snow product resolution. Forests were defined by pixels with forest cover of at least 20%. Burned area was determined using fire perimeter spatial data from the Geospatial Multi-Agency Coordination Group (GEOMAC) data distribution site [*Walters et al*., 2008] for 2000–2012.

4. Results and Discussion

4.1. Postfire Snow Spectral Albedo and Net Radiation

[13] During the accumulation period, the burned and unburned forests showed no difference in albedo (as measured with ASD-FR and pyranometers; Figures 4 and 5). Because of frequent snowfall events, the effect of BWD on albedo was negligible during this period. However, during the ablation period, BWD concentrated on the snowpack surface, decreasing snow albedo by 40%. Previous research has shown that particulates larger than 5 μm in diameter are typically not flushed downward through the snowpack with meltwater [*Conway et al*., 1996], and thus concentrate on the snowpack surface during ablation [*Painter et al*., 2012]. Throughout the accumulation (acc.) and ablation (abl.) periods, spectral albedo in the unburned forest maintained uniform spatial variability (acc. 0.74 ± 0.02, abl. 0.58 ± 0.02), while the temporal variability of broadband albedo increased during ablation (acc. 0.67 ± 0.13, abl. 0.38 ± 0.18). Spectral albedo in the burned forest maintained uniform spatial variability (acc. 0.75 ± 0.04, abl. 0.42 ± 0.05), while the temporal variability of broadband albedo decreased (acc. 0.68 ± 0.08, abl. 0.28 ± 0.03) during ablation.

[14] Mean solar radiation incident on the snow surface was approximately 60% greater in the burned forest than in the unburned forest (Figure 5). Particularly in the unburned forest, the downward-facing pyranometers may have had trees in a portion of their field-of-view, thereby underestimating snow albedo. Also in the unburned forest, snow albedo was lower than for pristine snow due to deposition of forest litter. Our measurements were comparable with reported values [*Burles and Boon*, 2011; *Melloh et al*., 2002].

[15] In the burned forest, lower snow albedo combined with increased canopy transmissivity resulted in greater net shortwave radiation compared with the unburned forest (Table 1). During the accumulation period, net shortwave radiation was 60% greater in the burned forest. While during ablation, net shortwave radiation was over 200% greater in the burned forest. Spatial (Figure 4) and temporal (Figure 5) within-site variability in snow albedo, incoming solar radiation, and BWD concentrations, combined with fine-scale heterogeneity in snow dynamics [cf. *Jost et al*., 2007, and references therein], introduces uncertainty in the results, but is outweighed by large overall increases in net shortwave radiation.

4.2. Snow Debris Concentration and Spectral Reflectance Characterization

[16] Filtered snow samples collected in both plots during the accumulation period showed no significant differences in their respective debris concentrations (grams of debris per kilogram of snow). However, samples from the ablation period showed that the burned forest had more than double the mean debris concentration (UF: 2.4 ± 2.4 g/kg; BF: 7.1 ± 11.8 g/kg). Spectral reflectance factor measurements of filtered debris showed that the BWD samples had 25% lower reflectance than debris from the unburned forest snowpack (Figure 4). The greater concentration of darker debris in the burned forest suggests it had a greater radiative impact on snowmelt.

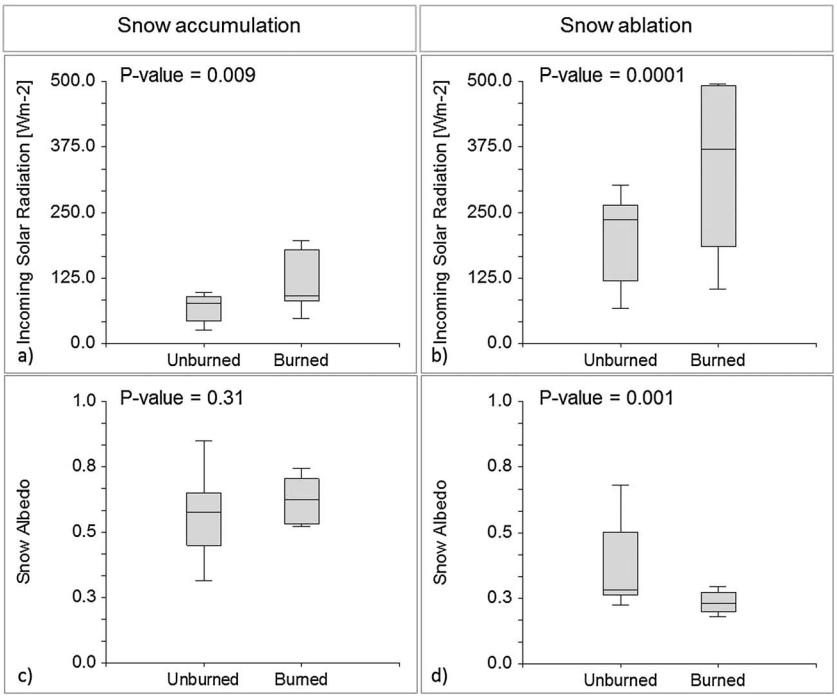

Figure 5. Box plots showing median and interquartile ranges in the distribution of pyranometer-measured incoming solar radiation during (a) snow accumulation (4–27 February 2012) and (b) snow ablation (8–31 May 2012); and snow albedo during (c) snow accumulation (4–27 February 2012), and (d) snow ablation (8–31 May 2012), in the burned and unburned forest plots.

[17] Although we did not explicitly quantify debris concentrations in proximity to trees, we noted that debris concentrations were highest near tree trunks. Our sampling strategy captured the range of spatial variability of spectral albedo and debris concentrations.

4.3. Forest Structure and Postfire Snow Dynamics

[18] In the burned forest, TLS data showed a 500% reduction in stem density (UF: one tree per 6.7 m^2; BF: one tree per 34.0 m^2). Hemispherical image analysis showed a 300% reduction in mean canopy density compared with the unburned forest (UF: 66 ± 5%; BF: 22 ± 4%). Snow survey results showed that the loss of overstory decreased canopy snow interception, thereby increasing snow accumulation on the ground. Maximum SWE was 11% greater in the burned forest (UF: 90 ± 21 cm; BF: 101 ± 29 cm), but it disappeared 23 days earlier than in the unburned forest (Figure 6). After the date of peak SWE, average snow ablation rate in the burned forest was almost twice as fast as in the unburned forest (UF: 1.2 cm d^{-1}; BF: 2.3 cm d^{-1}). The

Table 1. Changes in Net Shortwave Radiation Due to the Differences in Snow Albedo and Incoming Solar Radiation in Unburned and Burned Forest Plots[a]

Measurement Period	Measurement Type	Forest Type	Mean Snow Albedo	Mean Incoming Shortwave Radiation ($W m^{-2}$)	Net Shortwave Radiation ($W m^{-2}$)
Accumulation	Pyranometer	Unburned forest	0.67	69	23
		Burned forest	0.68	114	36
		Change in net shortwave radiation			13
Accumulation	ASD-FR	Unburned forest	0.75	69	17
		Burned forest	0.74	114	30
		Change in net shortwave radiation			13
Ablation	Pyranometer	Unburned forest	0.38	203	126
		Burned forest	0.29	363	258
		Change in net shortwave radiation			132
Ablation	ASD-FR	Unburned forest	0.58	203	85
		Burned forest	0.42	363	211
		Change in net shortwave radiation			126

[a]Pyranometer measured snow albedo and radiation values were calculated for the snow accumulation period (4-27 February 2012), and snow ablation period (8-31 May 2012). ASD-FR measured snow albedo values were calculated for the snow accumulation period (25 March 2013), and snow ablation period (4 May 2012).

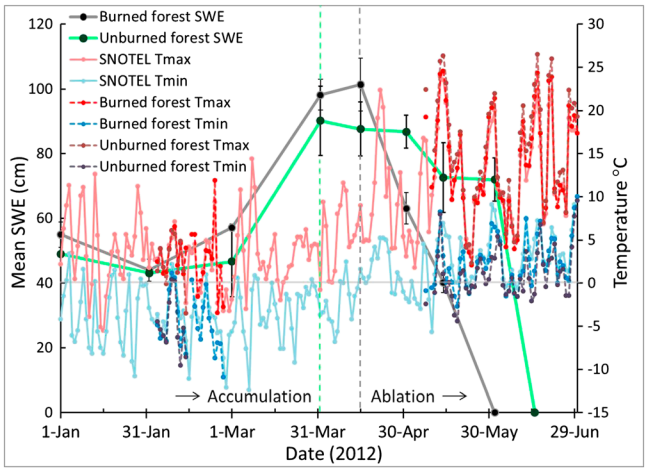

Figure 6. Measured mean snow water equivalent (SWE) in burned and unburned forests. Maximum SWE is indicated by vertical dashed lines. Minimum and maximum temperature data in burned and unburned forests, and retrieved from nearby NRCS-SNOTEL Hogg Pass Site. Horizontal grey line indicates 0°C.

snowpack in the unburned forest disappeared 75 days after the date of peak SWE, whereas the snowpack in the burned forest disappeared in 47 days, over 60% faster.

4.4. Fire in the Seasonal Snow Zone in the Western United States

[19] Our spatial analysis demonstrated that from 2000–2012, over 80% of forest fires in the western U.S. burned in the seasonal snow zone (Figure 7). These forest fires in the seasonal snow zone were 4.4 times larger than those outside the seasonal snow zone. Since 2000, over 44,000 km^2 of forests in the seasonal snow zone have burned. These snow-dominated headwater catchments in the western U.S. are likely being influenced by the postfire snow albedo/canopy transmissivity effect. The relative importance of this effect will vary across scales with snow climate [*Sturm et al.*, 1995], forest type, and burn severity. From a large watershed perspective, we note that in the western U.S., nearly half (48%) of all forest fires in the seasonal snow zone lie within the Columbia River Basin of the Pacific Northwest.

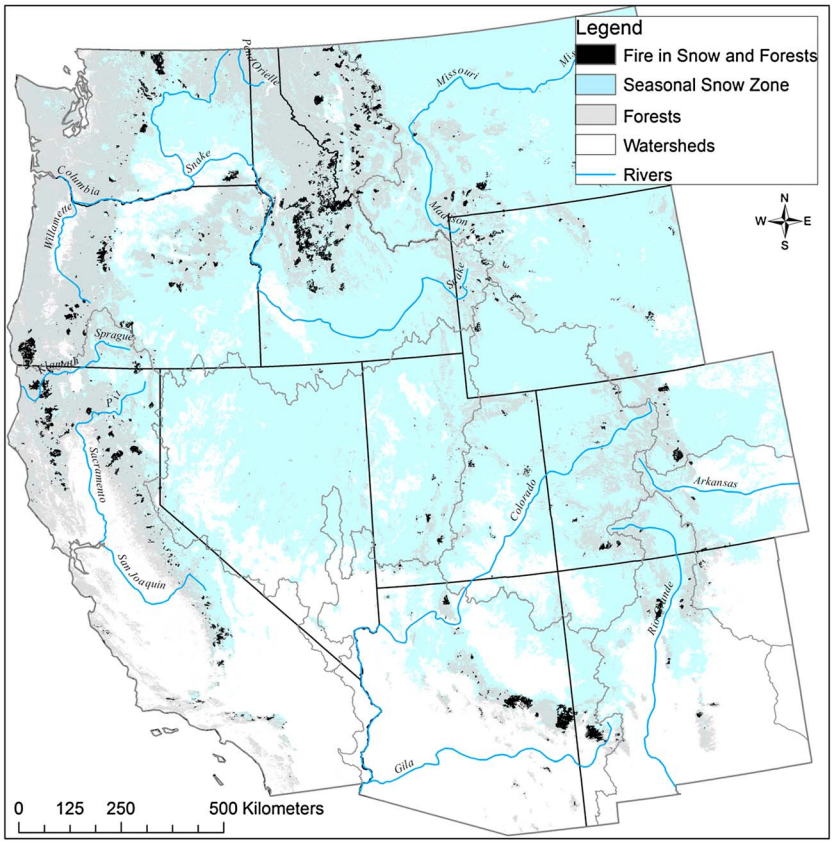

Figure 7. Forest fire area overlapping the seasonal snow zone in the western United States (2000–2012).

5. Conclusions

[20] While the competing effects of increased snow accumulation and increased snow ablation rate have been previously documented in fire-affected watersheds [*Burles and Boon*, 2011; *Harpold et al*., 2013; *Pomeroy et al*., 2012; *Skidmore et al*., 1994; *Winkler*, 2011], this study was the first to address the additional forcing of earlier melt due to the effects of BWD on snow albedo. The snowpack surface, darkened with the concentrated BWD, was primed to absorb more than double the incoming solar radiation.

[21] While this study addressed first year postfire effects on snow albedo and incoming solar radiation, the longer-term effects remain unclear. Studies have shown that burned forests remain standing for decades after fire disturbance depending on forest composition, forest structure, and burn severity [*Acker et al*., 2013; *Bigler and Veblen*, 2011; *Dunn and Bailey*, 2012]. Previous work estimated a half-life of standing burned fine-fuels ($\leq$23 cm) to be approximately 10 years [*Dunn and Bailey*, 2012]. As long as charred trees remain standing, they can contribute BWD to the snowpack surface. Six years after a fire, *Burles and Boon* [2011] measured higher snow albedo values in a burned forest than in a control forest. Eventually, snow in burned forests will have less debris and therefore higher albedo compared with unburned forests, thereby reducing net solar radiation at the snowpack surface. Until forest regeneration, their radiation balance may resemble that of an alpine snowpack above treeline. Such conjecture invites further investigation such as longer-term studies in burned forest stands of different postfire ages.

[22] Paradoxically, by removing the dark forest canopy and exposing the underlying snow cover, wildfire increases the overall winter/spring albedo of the land surface, creating a negative atmospheric radiative forcing [*Chambers et al*., 2005; *Chapin et al*., 2000; *O'Halloran et al*., 2012]. However, from the perspective of the snowpack, the albedo is decreased following a wildfire, and subsequent radiative heating and accelerated melt may have ecohydrological implications for forested snow-dominated headwater catchments [*Kelly and Goulden*, 2008].

[23] As climate continues to change, fire extent and severity are likely to increase across catchments of the mountain West [*Moritz et al*., 2012]. The "new normal" of increasingly large high-severity forest fires will have implications for changes in the amount and timing of snowmelt runoff in the western U.S.

[24] **Acknowledgments.** Data were provided by the GeoMAC Data Distribution Site and the National Snow and Ice Data Center (NSIDC). This work was supported by a NSF Hydrologic Sciences Rapid grant (1213612) and a NSF Water Sustainability and Climate award (EAR-1039192). We thank the OSU Geomatics Group for conducting the TLS surveys, and the OSU Mountain Hydroclimatology Research Group for assisting with snow surveys.

[25] The Editor thanks Jessica Lundquist and an anonymous reviewer for their assistance in evaluating this paper.

References

Abatzoglou, J. T. (2011), Influence of the PNA on declining mountain snowpack in the Western United States, *Int. J. Climatol.*, *31*(8), 1135–1142.

Acker, S. A., J. Kertis, H. Bruner, K. O'Connell, and J. Sexton (2013), Dynamics of coarse woody debris following wildfire in a mountain hemlock (*Tsuga mertensiana*) forest, *For. Ecol. Manage.*, *302*, 231–239.

Bigler, C., and T. T. Veblen (2011), Changes in litter and dead wood loads following tree death beneath subalpine conifer species in northern Colorado, *Can. J. Forest Res.*, *41*(2), 331–340.

Brown, R. D., and P. W. Mote (2009), The response of Northern Hemisphere snow cover to a changing climate, *J. Climate*, *22*(8), 2124–2145.

Burles, K., and S. Boon (2011), Snowmelt energy balance in a burned forest plot, Crowsnest Pass, Alberta, Canada, *Hydrolog. Process.*, *25*(19), 3012–3029.

Chambers, S. D., J. Beringer, J. T. Randerson, and F. S. Chapin (2005), Fire effects on net radiation and energy partitioning: Contrasting responses of tundra and boreal forest ecosystems, *J. Geophys. Res.*, *110*, D09106, doi: 10.1029/2004JD005299.

Chapin, F. S., et al. (2000), Arctic and boreal ecosystems of western North America as components of the climate system, *Glob. Chang. Biol.*, *6*, 211–223.

Conway, H., A. Gades, and C. Raymond (1996), Albedo of dirty snow during conditions of melt, *Water Resour. Res.*, *32*(6), 1713–1718.

DiMiceli, C. M., M. L. Carroll, R. A. Sohlberg, C. Huang, M. C. Hansen, and J. R. G. Townshend (2011), *Vegetation Continuous Fields MOD44B*, U. o. Maryland, College Park, Maryland.

Dozier, J., R. O. Green, A. W. Nolin, and T. H. Painter (2009), Interpretation of snow properties from imaging spectrometry, *Remote Sens. Environ.*, *113*, S25–S37.

Dunn, C. J., and J. D. Bailey (2012), Temporal dynamics and decay of coarse wood in early seral habitats of dry-mixed conifer forests in Oregon's Eastern Cascades, *For. Ecol. Manage.*, *276*, 71–81.

Flanner, M. G., C. S. Zender, P. G. Hess, N. M. Mahowald, T. H. Painter, V. Ramanathan, and P. J. Rasch (2009), Springtime warming and reduced snow cover from carbonaceous particles, *Atmos. Chem. Phys.*, *9*(7), 2481–2497.

Franklin, J. F., and C. Dyrness (1973), *Natural vegetation of Oregon and Washington*, Oregon State University Press, Corvallis, Oregon, USA.

Frazer, G., C. Canham, and K. Lertzman (1999), Gap Light Analyzer (GLA): Imaging software to extract canopy structure and gap light transmission indices from true-colour fisheye photographs: User's manual and program documentation, Simon Fraser University, Burnaby, BC. [doi:10.1016/S0168-1923(01)00274-X].

Hall, D. K., G. A. Riggs, and V. V. Salomonson (2006), *MODIS/Terra Snow Cover 8-day L3 Global 500 m Grid V005*, N. S. a. I. D. Center, Boulder, Colorado.

Hardy, J., R. Melloh, P. Robinson, and R. Jordan (2000), Incorporating effects of forest litter in a snow process model, *Hydrolog. Process.*, *14*(18), 3227–3237.

Harpold, A. A., J. A. Biederman, K. Condon, M. Merino, Y. Korgaonkar, T. Nan, L. L. Sloat, M. Ross, and P. D. Brooks (2013), Changes in snow accumulation and ablation following the Las Conchas Forest Fire, New Mexico, USA, *Ecohydrology*, doi:10.1002/eco.1363.

Jost, G., M. Weiler, D. R. Gluns, and Y. Alila (2007), The influence of forest and topography on snow accumulation and melt at the watershed-scale, *J. Hydrol.*, *347*(1-2), 101–115.

Kelly, A. E., and M. L. Goulden (2008), Rapid shifts in plant distribution with recent climate change, *Proc. Natl. Acad. Sci. U. S. A.*, *105*(33), 11,823–11,826.

Knowles, N., M. D. Dettinger, and D. R. Cayan (2006), Trends in snowfall versus rainfall in the Western United States, *J. Climate*, *19*(18), 4545–4559.

Littell, J. S., D. McKenzie, D. L. Peterson, and A. L. Westerling (2009), Climate and wildfire area burned in western U. S. ecoprovinces, 1916–2003, *Ecol. Appl.*, *19*(4), 1003–1021.

Marlon, J. R., et al. (2012), Long-term perspective on wildfires in the western USA, *Proc. Natl. Acad. Sci. U. S. A.*, *109*(9), E535–E543.

Melloh, R. A., J. P. Hardy, R. E. Davis, and P. B. Robinson (2001), Spectral albedo/reflectance of littered forest snow during the melt season, *Hydrolog. Process.*, *15*(18), 3409–3422.

Melloh, R. A., J. P. Hardy, R. N. Bailey, and T. J. Hall (2002), An efficient snow albedo model for the open and sub-canopy, *Hydrolog. Process.*, *16*(18), 3571–3584.

Moritz, M. A., M.-A. Parisien, E. Batllori, M. A. Krawchuk, J. Van Dorn, D. J. Ganz, and K. Hayhoe (2012), Climate change and disruptions to global fire activity, *Ecosphere*, *3*(6), art49.

Mote, P. W., A. F. Hamlet, M. P. Clark, and D. P. Lettenmaier (2005), Declining mountain snowpack in western North America, *Bull. Am. Meteorol. Soc.*, *86*(1), 39–49.

O'Halloran, T. L., et al. (2012), Radiative forcing of natural forest disturbances, *Glob. Chang. Biol.*, *18*(2), 555–565.

Painter, T. H., A. P. Barrett, C. C. Landry, J. C. Neff, M. P. Cassidy, C. R. Lawrence, K. E. McBride, and G. L. Farmer (2007), Impact of disturbed desert soils on duration of mountain snow cover, *Geophys. Res. Lett.*, *34*, L12502, doi:10.1029/2007GL030284.

Painter, T. H., A. C. Bryant, and S. M. Skiles (2012), Radiative forcing by light absorbing impurities in snow from MODIS surface reflectance data, *Geophys. Res. Lett.*, *39*, L17502, doi:10.1029/2012GL052457.

Pederson, G. T., J. L. Betancourt, and G. J. McCabe (2013), Regional patterns and proximal causes of the recent snowpack decline in the Rocky Mountains, US, *Geophys. Res. Lett.*, *40*, 1811–1816, doi:10.1002/grl.50424.

Pomeroy, J., X. Fang, and C. Ellis (2012), Sensitivity of snowmelt hydrology in Marmot Creek, Alberta, to forest cover disturbance, *Hydrolog. Process.*, *26*(12), 1892–1905.

Preston, C., and M. Schmidt (2006), Black (pyrogenic) carbon: A synthesis of current knowledge and uncertainties with special consideration of boreal regions, *Biogeosciences*, *3*(4), 397–420.

Robinson, D. A., and A. Frei (2000), Seasonal variability of Northern Hemisphere snow extent using visible satellite data, *The Professional Geographer*, *52*(2), 307–315.

Serreze, M. C., M. P. Clark, R. L. Armstrong, D. A. McGinnis, and R. S. Pulwarty (1999), Characteristics of the western United States snowpack from snowpack telemetry (SNOTEL) data, *Water Resour. Res.*, *35*(7), 2145–2160.

Skidmore, P., K. Hansen, and W. Quimby (1994), *Snow accumulation and ablation under fire-altered lodgepole pine forest canopies*, in Proceedings, 62nd Western Snow Conference, Santa Fe, N.M., U.S.A. pp. 43–52.

Skiles, S. M., T. H. Painter, J. S. Deems, A. C. Bryant, and C. C. Landry (2012), Dust radiative forcing in snow of the Upper Colorado River Basin: 2. Interannual variability in radiative forcing and snowmelt rates, *Water Resour. Res.*, *48*, W07522, doi:10.1029/2012WR011986.

Sturm, M., J. Holmgren, and G. E. Liston (1995), A seasonal snow cover classification system for local to global applications, *J. Climate*, *8*(5), 1261–1283.

Taylor, G., and C. Hannan (1999), *The climate of Oregon: From rain forest to desert*, 211 pp., Oregon State University Press, Corvallis, Oregon.

Walters, S. P., N. J. Schneider, and J. D. Guthrie (2008), Geospatial Multi-Agency Coordination (GeoMAC) wildland fire perimeters.

Warren, S. G., and W. J. Wiscombe (1980), A model for the spectral albedo of snow, 2. Snow containing atmospheric aerosols, *J. Atmos. Sci.*, *37*(12), 2734–2745.

Westerling, A. L., H. G. Hidalgo, D. R. Cayan, and T. W. Swetnam (2006), Warming and earlier spring increase western U.S. forest wildfire activity, *Science*, *313*(5789), 940.

Westerling, A. L., B. P. Bryant, H. K. Preisler, T. P. Holmes, H. G. Hidalgo, T. Das, and S. R. Shrestha (2011), Climate change and growth scenarios for California wildfire, *Clim. Change*, *109*, 445–463.

Winkler, R. D. (2011), Changes in snow accumulation and ablation after a fire in south-central British Columbia, *Streamline Watershed Manag. Bull.*, *14*(2), 1–7.